PHOTONICS Research

Extraction of internal phase motions in femtosecond soliton molecules using an orbital-angular-momentum-resolved method

Yuwei Zhao,[1,†] Jintao Fan,[2,3,†] Youjian Song,[1,5] Uwe Morgner,[2,3,4] and Minglie Hu[1,6]

[1]Ultrafast Laser Laboratory, Key Laboratory of Opto-electronic Information Science and Technology of Ministry of Education, School of Precision Instruments and Opto-electronics Engineering, Tianjin University, Tianjin 300072, China
[2]Institut für Quantenoptik, Leibniz Universität Hannover, Welfengarten 1, 30167 Hannover, Germany
[3]Cluster of Excellence PhoenixD (Photonics, Optics, and Engineering-Innovation Across Disciplines), 30167 Hannover, Germany
[4]Laser Zentrum Hannover e.V., Hollerithallee 8, 30419 Hannover, Germany
[5]e-mail: yjsong@tju.edu.cn
[6]e-mail: huminglie@tju.edu.cn

Received 2 June 2020; revised 30 July 2020; accepted 1 August 2020; posted 4 August 2020 (Doc. ID 398316); published 18 September 2020

Internal motions in femtosecond soliton molecules provide insight into universal collective dynamics in various nonlinear systems. Here we introduce an orbital-angular-momentum (OAM)-resolved method that maps the relative phase motion within a femtosecond soliton molecule into the rotational movement of the interferometric beam profile of two optical vortices. By this means, long-term relative phase evolutions of doublet and triplet soliton molecules generated in an all-polarization-maintaining mode-locked Er-fiber laser are revealed. This simple and practical OAM-resolved method represents a promising way to directly visualize the complex phase dynamics in a diversity of multisoliton structures.

https://doi.org/10.1364/PRJ.398316

1. INTRODUCTION

Optical solitons in femtosecond lasers play an important role in the study of solitary wave propagation and interaction effects that are universal in a variety of research fields, ranging from fluid and condensed matter physics to chemistry and neurobiology [1,2]. It is generally recognized that dissipative soliton formation is responsible for ultrashort pulse shaping and stabilization in laser cavities [3–5]. In particular, interactions between individual dissipative solitons lead to various bound states, which are frequently referred to as soliton molecules [6]. Since their early observation, soliton molecules have attracted tremendous attention due to their potential to upgrade the transmission capability of optical communication [7,8] and to demonstrate complex soliton interaction behaviors in dynamical nonlinear systems [6,9–14].

In optical soliton molecules, the internal motions between solitons turn out to have two degrees of freedom, namely, the binding separation and relative phase between two solitons [6,15,16]. Stationary femtosecond soliton molecules with constant binding separation and relative phase have long been proved to exist in various laser configurations by optical spectral analysis, while the time-averaged measurements based on optical spectral analyzers hinder the observation of more complex soliton molecular dynamics [17–19]. Recently, various real-time spectroscopic techniques as well as time-domain probes [20–22] have been proposed to address this problem. In particular, a time-stretch dispersive Fourier transform (DFT) technique has been frequently utilized to unveil the shot-to-shot evolution of soliton molecular spectra [23–30], enabling the identification of different kinds of vibrating and oscillating modes in soliton molecules [2,23–25,31,32]. While the DFT technique is very appealing for probing the transient properties within soliton molecules, the observation time frame is limited to hundreds of microseconds (corresponding to tens of thousands of round-trips), mainly confined by the storage capability of the real-time oscilloscopes.

In this paper, we experimentally demonstrate a new probing concept, an orbital-angular-momentum (OAM)-resolved method, for visual extraction of long-term internal phase motions within soliton molecules produced by a mode-locked laser. We show that temporally varying phases within soliton molecules can be transformed to the spatial phase difference between two optical vortices. As a consequence, by using a fast-frame-rate CCD camera to monitor the rotational movement of the combined vortices, the complex internal motion of soliton molecules in terms of relative phase evolution can be monitored over a long period. In a proof-of-principle experiment, two different kinds of soliton molecular phase properties, namely, stationary and monotonic phase evolutions, are characterized. This technique provides a practical, low-cost, and

simple diagnostic for internal phase dynamics within soliton complexes.

2. EXPERIMENTAL SETUP

The experimental setup of the proposed OAM-resolved method for relative phase characterization between the two bound pulses within soliton molecules is schematically illustrated in Fig. 1. A home-built nonlinear amplifying loop mirror (NALM) mode-locked all-polarization-maintaining (PM) Er-fiber laser is used as the platform for soliton molecular generation. The laser design is identical to our previous reported one [33] by simply excluding the vortex wave plate (VWP) inside the laser cavity. Soliton bound states with different binding separations can be obtained in a reproducible way by fine adjustments of pump power and laser output ratio. The inset shows a diagram of a twin-pulse molecule, where the relative phase within the molecule is sketched. The soliton molecular pulse train emitted by the laser is directed to the OAM-resolved monitoring system. The working principle of this method will be explained in more detail hereafter. Essentially, we utilize a commercially available CCD (Bobcat-320, Xenics) to record a sequence of images at a capturing rate of one frame per five seconds for tracking the long-term variation of the relative phase difference between the two bound pulses within the soliton molecules.

It has been demonstrated that optical vortices can be utilized to map the temporal phase difference into spatial dimension, providing spatiotemporal phase manipulation capacity for optical frequency combs [34,35] and related spectroscopic applications. Here we take advantage of this property of optical vortices, for the first time to our knowledge, to retrieve internal phase motions in femtosecond soliton molecules, which is referred to as an OAM-resolved method. Specifically, this technique is based on interference of two optical vortices with opposite topological charges ($l_1 = 1$ and $l_2 = -1$). Note that the precision of the interferometric process strongly relies on temporal overlap. To this end, the bound soliton pairs are sent to a Mach–Zehnder-like interferometer (MZI), where the front pulse and the rear pulse are split, delayed, and then recombined as shown in Fig. 1. The time delay set in one arm allows us to finely tune the optical path difference and thus leads to a delicate overlap between the two bound pulses by using the autocorrelation trace as the monitor. It should be pointed out that

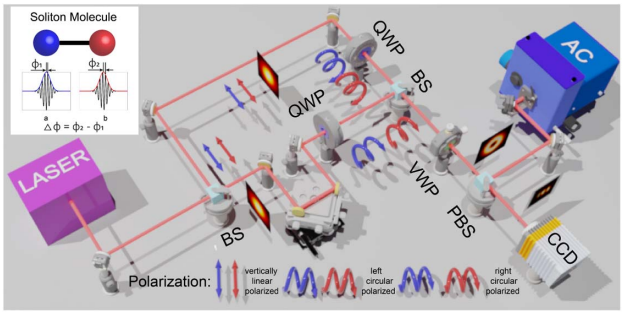

Fig. 1. Experimental setup. AC, autocorrelator; BS, beam splitter; PBS, polarization beam splitter; QWP, quarter-wave plate; VWP, vortex wave plate. The inset shows the diagram of a twin-pulse molecule.

environmental noises result in differential length fluctuations between the two arms of the MZI and thus result in a phase fluctuation. To minimize the environmental noises, a highly stable translation stage is employed, and the two arm lengths are set to be as short as possible.

A quarter-wave plate (QWP) is inserted into each arm of the MZI, and it translates the vertically linearly polarized output pulses from the mode-locked laser into circular polarization. The slow axes of the two QWPs are vertically placed so that the outputs from the two arms of the MZI show opposite circular polarization. The combined beams pass through a VWP (Thorlabs WPV10L-1550) in the following, and thus two optical vortices with opposite topological charges are produced. The superposition of the two optical vortices results in a cylindrical vector beam (CVB) [36–38] whose state can be described as

$$e^{\frac{-i\Delta\phi}{2}}\begin{bmatrix}\cos\left(\phi+\frac{\Delta\phi}{2}\right)\\ \sin\left(\phi+\frac{\Delta\phi}{2}\right)\end{bmatrix}, \tag{1}$$

where $\frac{\Delta\phi}{2}$ is the phase difference between the optics vortices with topological charges $l_1 = 1$ and $l_2 = -1$, which is the relative phase of soliton molecule under test, and ϕ is the initial phase of the CVB, which is introduced by MZI and can be obtained in advance by using a single pulse as the input of the MZI, where $\Delta\phi = 0$. Figure 2(a) illustrates the procedure to produce a cylindrical vector beam by superposition of two optical vortices with opposite topological charges. A simple numerical simulation has been conducted here to better

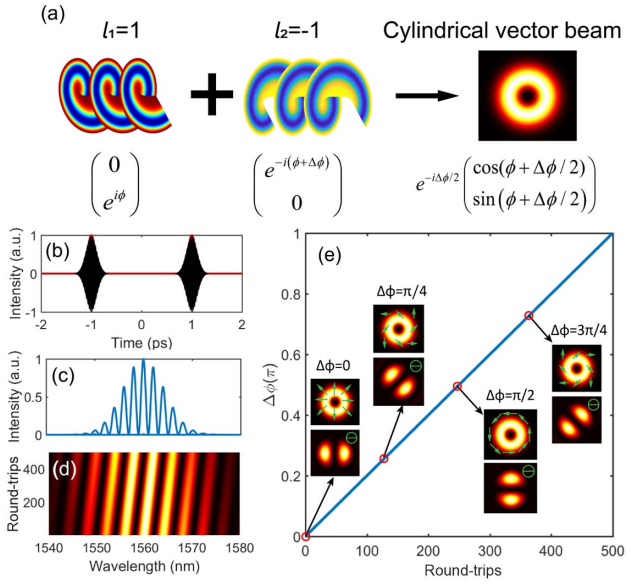

Fig. 2. Principle of the OAM-resolved method. (a) Interference pattern created by two optical vortices with topological charges $l_1 = 1$ and $l_2 = -1$; (b), (c) temporal and spectral properties of a simulated soliton molecule; (d) simulated spectral evolution over 500 round-trips in consideration of linear relative phase evolution; (e) the phase evolution retrieved from (d) and the corresponding interferometric patterns. Arrows are used to indicate the polarization distributions in each case. The lobes present the results measured behind a horizontal polarizer.

understand the working principle of the OAM-resolved method. Figures 2(b) and 2(c) present the time-domain and spectral-domain profiles of a simulated twin-pulse soliton molecule centered at 1560 nm with a temporal separation of 2 ps, respectively. The relative phase within the molecule evolves linearly with cavity round-trip time. Figure 2(d) shows the evolving interferometric optical spectra over 500 round-trips. Figure 2(e) shows the linear phase evolution retrieved from Fig. 2(d) and the interferometrical patterns of cylindrical vector beams based on the OAM-resolved method. Four typical cylindrical vector beams with different $\Delta\phi$ are shown here. The lobe structures illustrate the corresponding beam profiles after passing a polarization beam splitter. The two-lobe pattern rotates around its own central null with the increase of $\Delta\phi$ [39]. At this point, the phase difference within soliton molecules is mapped into rotation direction of an interferometric pattern. In turn, the phase motions within soliton molecules can be read out from the dynamical rotation of the interferometric pattern. To obtain the relative phase within a soliton molecule, we need to extract the axis that the interferometric lobes would rotate about. Similar to the least-squares solution method [40], which is derived for estimating the average center and the axis of rotation of 3D motion data, the following procedures are taken: (i) the intensity distribution of the mode field is represented as $I(x,y)$; (ii) we define the moment of the mode field about an arbitrary axis $ax+by+c=0$ as $d=u(a,b,c)$; (iii) we minimize the moment $u(a,b,c)$, and therefore, the line (axis) in the Visualization 1 is obtained; (iv) the slope of the axis $\theta=\arctan(-\frac{a}{b})$ is calculated. The extraction process of θ described above can be given as follows:

$$\begin{aligned} &\min u(a,b,c),\\ &u(a,b,c)=\iint |d(x,y)|^2 I(x,y)\mathrm{d}x\mathrm{d}y,\\ &|d(x,y)|^2=\tfrac{(ax+by+c)^2}{a^2+b^2},\\ &\theta=\arctan(-\tfrac{a}{b}). \end{aligned} \tag{2}$$

The validity of this algorithm is shown in Visualization 1, where accurate θ extraction over 180 deg rotation of the two-lobe interferometric pattern is represented.

3. RESULTS AND DISCUSSION

With fine adjustment of waveplate angles, a stable single-pulse mode-locking state is obtained with pulse repetition rate of 80 MHz when the pump power is well above the threshold pump power. The laser operates at the anomalous dispersion regime with a net cavity dispersion estimated to be -0.0096 ps^2. The pulse duration of the single soliton is 170 fs. Then the soliton molecular regime can be achieved by further increase of the pump power beyond a critical level. Since soliton molecule generation in a laser cavity relies on a dissipative mode-locking process, soliton molecules with various phase evolution states can be stimulated by means of changing the output coupling ratio and the pump power.

A. Stationary Soliton Molecule

First, a stationary twin-soliton molecule with locked relative phase is observed. The optical spectrum features a high-contrast interferometric pattern as depicted in Fig. 3(a). The 10 nm

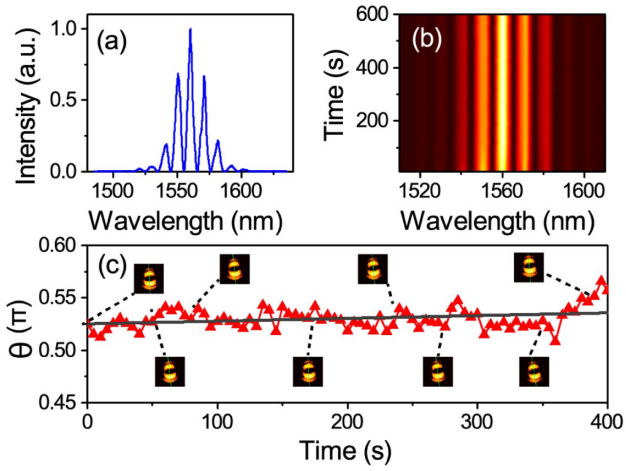

Fig. 3. Stationary soliton molecule. (a) Spectrum of the twin-soliton molecule, (b) spectral evolution over 10 min, (c) relative phase evolution of two soliton pulses within the soliton pairs within 400 s. The insets show the interferometric patterns after PBS.

modulation period in the spectrum corresponds to a binding separation of 800 fs, which is verified by the autocorrelation trace. Figure 3(b) shows the measured spectral evolution over 10 min by using the optical spectrum analyzer. The acquisition time for each spectrum is 8 s. Figure 3(c) presents the relative phase evolution within the soliton molecules over 400 s based on the OAM-resolved method. The relative phase has been retrieved by the angle of the two-lobe interferometric pattern displayed on the CCD. The exposure time for obtaining each beam profile is as short as 5.6 μs. The inset shows selected interferometric patterns, and no obvious rotation in their angles is observed. The solid line in Fig. 3(c) shows the linear fit of the 400 s relative phase evolution. There is a slight fluctuation around the averaged 0.53π relative phase with a standard deviation of 0.01π. Note that this relative phase contains both the soliton molecular relative phase and the initial phase of the MZI. The initial phase of the MZI is predetermined as 0.5π with a standard error of 0.001π by conducting the OAM-resolved measurement under a single-pulse mode-locking state (not provided here). Therefore, we obtain the relative phase within soliton molecule by applying $\theta=\Delta\phi+\pi/2$, where θ is the relative phase retrieved based on the OAM-resolved method and $\Delta\phi$ is the relative phase between the bounded soliton pairs. The relative phase within the soliton molecule is calculated to be 0.03π, which agrees well with that retrieved from the modulated optical spectrum.

B. Soliton Molecules with Monotonically Evolving Phase

Next, by carefully adjusting the output ratio and changing the pump power, we further resolve several soliton molecule states with monotonically evolving phase based on the OAM-resolved method as shown in Figs. 4(b), 4(d), 4(f), and 4(h). Figures 4(a), 4(c), 4(e), and 4(g) display the corresponding measured spectra over 10 min with a standard grating spectrometer, showing soliton molecular binding separations of 0.8, 1.4, 1.8, and 4 ps, respectively. Note that the 2D contour

plots obtained by an optical spectral analyzer fail to unveil the evolving relative phase over time due to the long integration time. The monotonically evolving phase observed with the OAM-resolved method can be attributed to slightly different amplitudes within the doublet soliton molecule. When propagating in each cavity round-trip, the amplitude difference can be converted to different carrier envelope phase shift, which leads to a long-term evolution of the relative phase [24,41]. Figures 4(b), 4(d), and 4(f) show that the slope of phase evolution over time flattens with the increase of pulse separation, and then it changes its sign. As is evident from these three figures, there shows a "turning point," which has been observed earlier in Ref. [23] and interpreted as a consequence of soliton attraction and repelling interactions. This law of motion does not apply to Fig. 4(h) because the pulse separation is too large, leading to a much weaker interaction between two solitons.

The evolution of the CCD-recorded interferometric patterns corresponding to Figs. 4(b), 4(d), 4(f), and 4(h) is plotted in Figs. 5(a)–5(d), respectively. At each binding separation, an apparent rotational movement of the two-lobe pattern is visible due to the constant variation of the soliton molecular phase difference. The rotation directions are also different for different binding separations, indicating distinct soliton interaction behaviors.

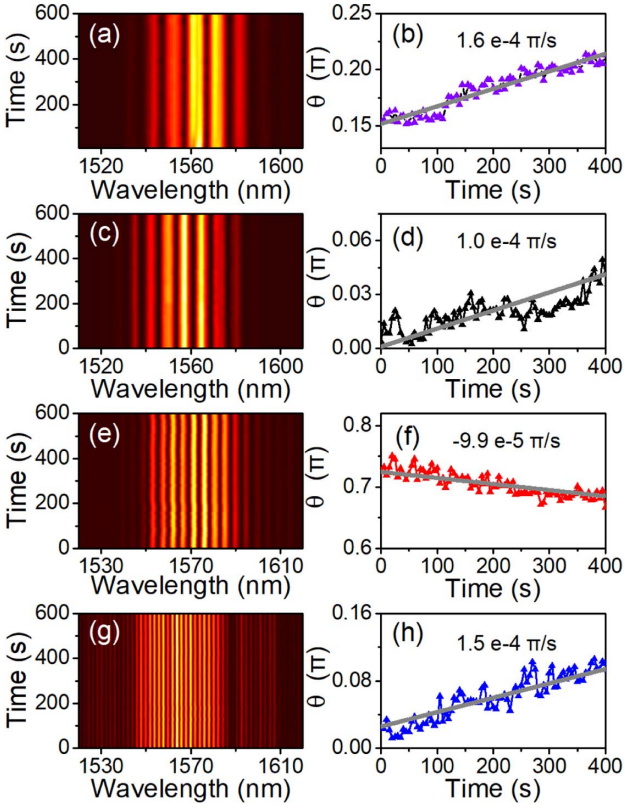

Fig. 4. Soliton molecules with monotonically evolving phase difference. Recorded spectra over 10 min with different pulse separations of (a) 0.8 ps, (c) 1.4 ps, (e) 1.8 ps, and (g) 4 ps. (b), (d), (f), and (h) The corresponding relative phase dynamics versus time.

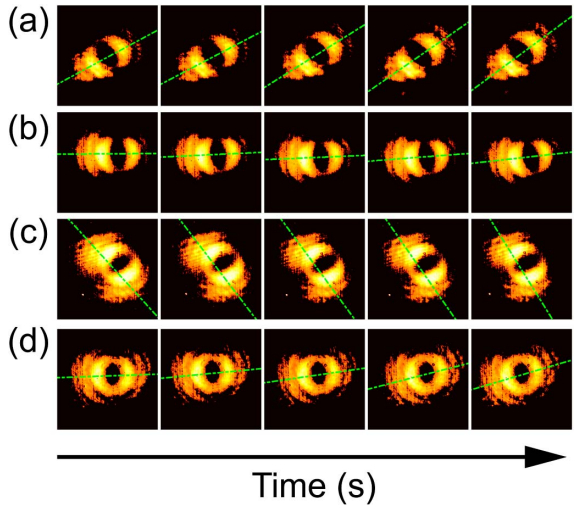

Fig. 5. Interferometric patterns recorded after PBS for different pulse separations of (a) 0.8 ps, (b) 1.4 ps, (c) 1.8 ps, and (d) 4 ps.

C. Soliton Molecule with Triplet Pulses

By further increasing the pump power, a soliton molecular state with equally spaced triplet pulses can be also observed, which is shown in Fig. 6. Figure 6(a) presents the optical spectrum. A series of spectra are recorded over 10 min as displayed in Fig. 6(b). The spectral modulation period is 8 nm, corresponding to a binding separation of 1 ps for neighboring pulses, which is further confirmed by the autocorrelation trace in Fig. 6(c). Here the relative phase between the leading soliton and center soliton is denoted by $\Delta\phi_{12}$, the relative phase between the leading (center) soliton and trailing soliton is denoted by $\Delta\phi_{13}$ ($\Delta\phi_{23}$), and the corresponding retrieved relative phases based on OAM-resolved method are defined as θ_{12}, θ_{13}, and θ_{23}. By carefully adjusting the delay line to optimize the temporal overlap, the relative internal phase dynamics can be characterized. The red scatters in Fig. 6(d) show the

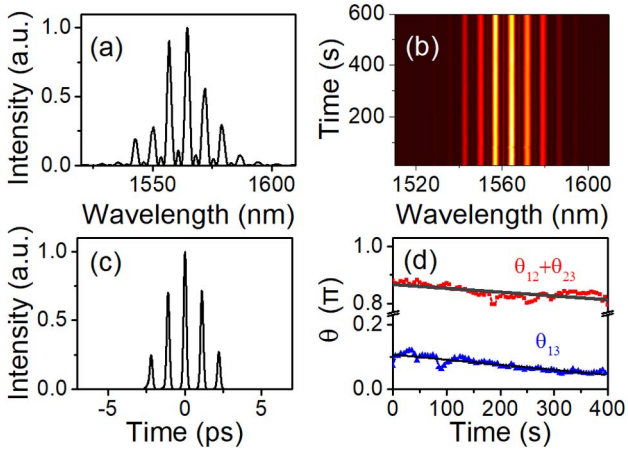

Fig. 6. Relative phase evolution within a tri-soliton molecule. (a) Spectrum of the tri-soliton molecule, (b) spectral intensity variation during 10 min, (c) autocorrelation trace of the tri-soliton molecule, (d) relative phase evolution of $\theta_{12}+\theta_{23}$ and θ_{13} based on the OAM-resolved method.

superposed relative phase variations of θ_{12} and θ_{23}. For comparison, the dynamics of θ_{13} (blue scatters) have also been recorded in Fig. 6(d). Note that the slopes are very similar when linearly fitting the variations of relative phase motions in the two cases, indicating $\Delta\phi_{13} = \Delta\phi_{12} + \Delta\phi_{23}$ (the initial phase has been subtracted here), which is typical for relative phase variation within triple-soliton molecules [30]. This finding reveals a monotonic relative phase variation of the three bound solitons, which is in good agreement with the observed molecule dynamics in Ref. [24].

4. CONCLUSION

To conclude, by means of the OAM-resolved method, we successfully resolve the long-term relative phase evolution of soliton molecules produced by a femtosecond Er-doped mode-locked fiber laser. Various soliton molecular states with stationary and monotonically evolving phase are characterized here. By translating the relative phase within a soliton molecule into the rotation of the interference pattern that is directly visible on a CCD, this method offers a simple and flexible alternative for tracking the relative phase dynamics within multisoliton complexes. Should a high-performance CCD (for example, 4 Quik E ICCD Camera, Stanford Computer Optics, Inc., ~1 ns exposure time) be used, it is possible to freeze a single-shot interferometric pattern for soliton molecules (even when the repetition rate is as high as ~1 GHz). Given that the OAM-resolved method is capable of transferring the temporal phase of soliton pairs to the spatial phase of vector beams, this technology holds the potential to trap and control the rotation of nanoparticles via manipulating soliton-molecular relative phases.

Funding. National Natural Science Foundation of China (61975144, 61827821, 11527808); The European Union's Horizon 2020 research and innovation programme under the Marie Sklodowska Curie grant (713694); The Deutsche Forschungsgemeinschaft (DFG) under Germany's Excellence Strategy within the Cluster of ExcellencePhoenixD (EXC 2122. ID: 390833453).

Acknowledgment. We thank the Key Laboratory of Opto-Electronics Information Technology in Tianjin University for the use of their equipment. We thank Dr. Fanchao Meng from Université Bourgogne Franche-Comté, Institut FEMTO-ST, Besançon, France for helpful discussion.

Disclosures. The authors declare no conflicts of interest.

†These authors contributed equally to this work.

REFERENCES

1. T. Dauxois and M. Peyrard, *Physics of Solitons* (Cambridge University, 2006).
2. K. Krupa, K. Nithyanandan, U. Andral, P. Tchofo-Dinda, and P. Grelu, "Real-time observation of internal motion within ultrafast dissipative optical soliton molecules," Phys. Rev. Lett. **118**, 243901 (2017).
3. P. Grelu and N. Akhmediev, "Dissipative solitons for mode-locked lasers," Nat. Photonics **6**, 84–92 (2012).
4. Y. Song, X. Shi, C. Wu, D. Tang, and H. Zhang, "Recent progress of study on optical solitons in fiber lasers," Appl. Phys. Rev. **6**, 021313 (2019).
5. M. Liu, Z. Wei, H. Li, T. Li, A. Luo, W. Xu, and Z. Luo, "Visualizing the 'invisible' soliton pulsation in an ultrafast laser," Laser Photon. Rev. **14**, 1900317 (2020).
6. N. N. Akhmediev, A. Ankiewicz, and J. M. Soto-Crespo, "Multisoliton solutions of the complex Ginzburg-Landau equation," Phys. Rev. Lett. **79**, 4047–4051 (1997).
7. L. Li, H. Huang, L. Su, D. Shen, D. Tang, M. Klimczak, and L. Zhao, "Various soliton molecules in fiber systems," Appl. Opt. **58**, 2745–2753 (2019).
8. M. Pang, W. He, X. Jiang, and P. St.J.Russell, "All-optical bit storage in a fibre laser by optomechanically bound states of solitons," Nat. Photonics **10**, 454–458 (2016).
9. N. Akhmediev, A. Ankiewicz, and J. Soto-Crespo, "Stable soliton pairs in optical transmission lines and fiber lasers," J. Opt. Soc. Am. B **15**, 515–523 (1998).
10. V. Afanasjev and N. Akhmediev, "Soliton interaction and bound states in amplified-damped fiber systems," Opt. Lett. **20**, 1970–1972 (1995).
11. H. Kitano and S. Kinoshita, "Stable multipulse generation from a self-mode-locked Ti:sapphire laser," Opt. Commun. **157**, 128–134 (1998).
12. F. M. Mitschke and L. F. Mollenauer, "Experimental observation of interaction forces between solitons in optical fibers," Opt. Lett. **12**, 355–357 (1987).
13. M. Stratmann, T. Pagel, and F. Mitschke, "Experimental observation of temporal soliton molecules," Phys. Rev. Lett. **95**, 143902 (2005).
14. R. Weill, A. Bekker, V. Smulakovsky, B. Fischer, and O. Gat, "Noise-mediated Casimir-like pulse interaction mechanism in lasers," Optica **3**, 189–192 (2016).
15. A. Hause, H. Hartwig, B. Seifert, H. Stolz, M. Böhm, and F. Mitschke, "Phase structure of soliton molecules," Phys. Rev. A **75**, 063836 (2007).
16. F. Meng, C. Lapre, C. Billet, G. Genty, and J. M. Dudley, "Instabilities in a dissipative soliton-similariton laser using a scalar iterative map," Opt. Lett. **45**, 1232–1235 (2020).
17. A. Haboucha, H. Leblond, M. Salhi, A. Komarov, and F. Sanchez, "Analysis of soliton pattern formation in passively mode-locked fiber lasers," Phys. Rev. A **78**, 043806 (2008).
18. A. Zavyalov, R. Iliew, O. Egorov, and F. Lederer, "Discrete family of dissipative soliton pairs in mode-locked fiber lasers," Phys. Rev. A **79**, 053841 (2009).
19. D. Tang, B. Zhao, L. Zhao, and H. Tam, "Soliton interaction in a fiber ring laser," Phys. Rev. E. **72**, 016616 (2005).
20. H. Shi, Y. Song, C. Wang, L. Zhao, and M. Hu, "Observation of sub-femtosecond fluctuations of the pulse separation in a soliton molecule," Opt. Lett. **43**, 1623–1626 (2018).
21. P. Ryczkowski, M. Närhi, C. Billet, J.-M. Merolla, G. Genty, and J. M. Dudley, "Real-time full-field characterization of transient dissipative soliton dynamics in a mode-locked laser," Nat. Photonics **12**, 221–227 (2018).
22. Y. Wei, B. Li, P. Feng, J. Kang, and K. K. Wong, "Broadband dynamic spectrum characterization based on gating-assisted electro-optic time lens," Appl. Phys. Lett. **114**, 021105 (2019).
23. M. Liu, H. Li, A. Luo, H. Cui, W. Xu, and Z. Luo, "Real-time visualization of soliton molecules with evolving behavior in an ultrafast fiber laser," J. Opt. **20**, 034010 (2018).
24. G. Herink, F. Kurtz, B. Jalali, D. R. Solli, and C. Ropers, "Real-time spectral interferometry probes the internal dynamics of femtosecond soliton molecules," Science **356**, 50–54 (2017).
25. X. Liu, X. Yao, and Y. Cui, "Real-time observation of the buildup of soliton molecules," Phys. Rev. Lett. **121**, 023905 (2018).
26. J. Peng and H. Zeng, "Build-up of dissipative optical soliton molecules via diverse soliton interactions," Laser Photon. Rev. **12**, 1800009 (2018).
27. S. Hamdi, A. Coillet, and P. Grelu, "Real-time characterization of optical soliton molecule dynamics in an ultrafast thulium fiber laser," Opt. Lett. **43**, 4965–4968 (2018).

28. Z. Wang, K. Nithyanandan, A. Coillet, P. Tchofo-Dinda, and P. Grelu, "Optical soliton molecular complexes in a passively mode-locked fibre laser," Nat. Commun. **10**, 830 (2019).
29. A. F. Runge, N. G. Broderick, and M. Erkintalo, "Observation of soliton explosions in a passively mode-locked fiber laser," Optica **2**, 36–39 (2015).
30. Y. Luo, R. Xia, P. P. Shum, W. Ni, Y. Liu, H. Q. Lam, Q. Sun, X. Tang, and L. Zhao, "Real-time dynamics of soliton triplets in fiber lasers," Photon. Res. **8**, 884–891 (2020).
31. X. Liu, D. Popa, and N. Akhmediev, "Revealing the transition dynamics from *Q* switching to mode locking in a soliton laser," Phys. Rev. Lett. **123**, 093901 (2019).
32. Y. Luo, J. Cheng, B. Liu, Q. Sun, L. Li, S. Fu, D. Tang, L. Zhao, and D. Liu, "Group-velocity-locked vector soliton molecules in fiber lasers," Sci. Rep. **7**, 2369 (2017).
33. Y. Zhao, J. Fan, H. Shi, Y. Li, Y. Song, and M. Hu, "Intracavity cylindrical vector beam generation from all-PM Er-doped mode-locked fiber laser," Opt. Express **27**, 8808–8818 (2019).
34. A. Asahara, S. Shoji, K. Kondo, Y. Wang, and K. Minoshima, "Coherent spatiotemporal phase control by combining optical frequency combs and optical vortices," in *CLEO: Science and Innovations* (Optical Society of America, 2018), paper STu4P–3.
35. A. Asahara, S. Shoji, and K. Minoshima, "Optical combs and optical vortices combined for spatiotemporal manipulation of light and matter," arXiv:2005.04705 (2020).
36. D. Naidoo, F. S. Roux, A. Dudley, I. Litvin, B. Piccirillo, L. Marrucci, and A. Forbes, "Controlled generation of higher-order Poincaré sphere beams from a laser," Nat. Photonics **10**, 327–332 (2016).
37. C. Yang, Z. Zhou, Y. Li, Y. Li, S. Liu, S. Liu, Z. Xu, G. Guo, and B. Shi, "Nonlinear frequency conversion and manipulation of vector beams in a Sagnac loop," Opt. Lett. **44**, 219–222 (2019).
38. J. T. Fan, J. Zhao, L. P. Shi, N. Xiao, and M. L. Hu, "Two-channel, dual-beam-mode, wavelength-tunable femtosecond optical parametric oscillator," Adv. Photon. **2**, 045001 (2020).
39. L. Paterson, M. P. MacDonald, J. Arlt, W. Sibbett, P. Bryant, and K. Dholakia, "Controlled rotation of optically trapped microscopic particles," Science **292**, 912–914 (2001).
40. S. S. H. U. Gamage and J. Lasenby, "New least squares solutions for estimating the average centre of rotation and the axis of rotation," J. Biomech. **35**, 87–93 (2002).
41. B. Ortaç, A. Zaviyalov, C. K. Nielsen, O. Egorov, R. Iliew, J. Limpert, F. Lederer, and A. Tünnermann, "Observation of soliton molecules with independently evolving phase in a mode-locked fiber laser," Opt. Lett. **35**, 1578–1580 (2010).